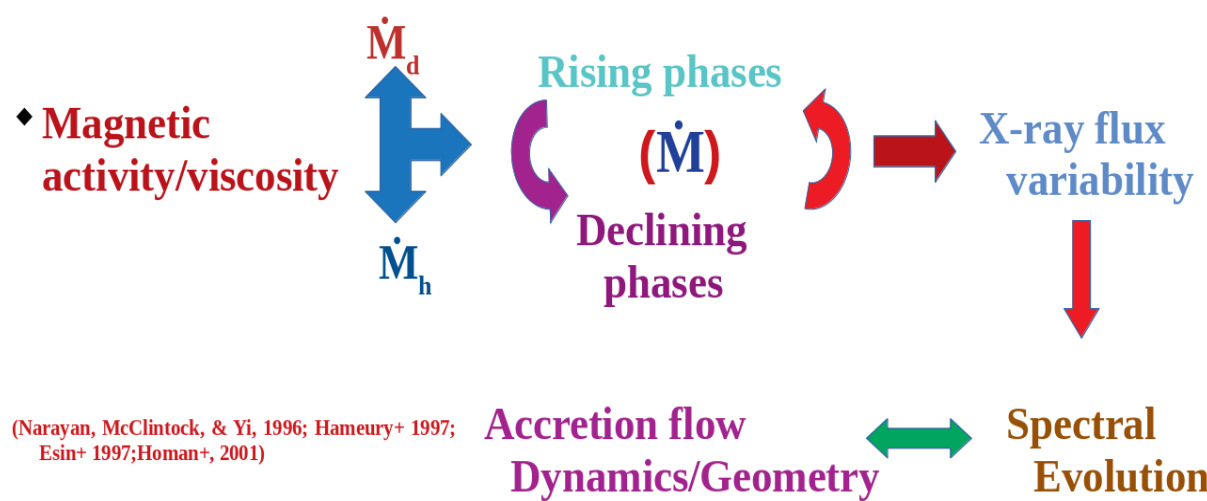


Accretion flow Geometry and Variations of Spectra-Temporal Parameters of a black hole candidate; MAXIJ1535-571

A. C. Eze & R. N. C. Eze

AFAS MARCH 20 - 27, 2026

Mass accretion rate (\dot{M}) variations/fluctuations during outburst evolution



T1 M4 RESULTS & DISCUSSION

Spectral Parameter/Units	MAXI-A	MAXI-B	MAXI-C
const	0.98	0.92	1.02
N_H/cm^{-2}	$(2.634 \pm 1.64) \times 10^{22}$	$(2.807 \pm 0.37) \times 10^{22}$	$(2.52 \pm 0.13) \times 10^{22}$
$m_{dot,d_TCAF}/M_{dot,d}$	0.548 ± 0.032	0.628 ± 0.001	0.721 ± 0.012
$m_{dot,h_TCAF}/M_{dot,h}$	$0.791^{+0.05}_{-0.05}$	0.737 ± 0.014	0.682 ± 0.201
m_{bb_TCAF}/M_O	9.674 ± 0.131	$8.901^{+0.32}_{-0.34}$	10.05 ± 0.191
X_S_TCAF/Γ_g	$56.214^{+0.061}_{-0.067}$	$48.284^{+1.022}_{-1.242}$	$46.475^{+1.011}_{-1.342}$

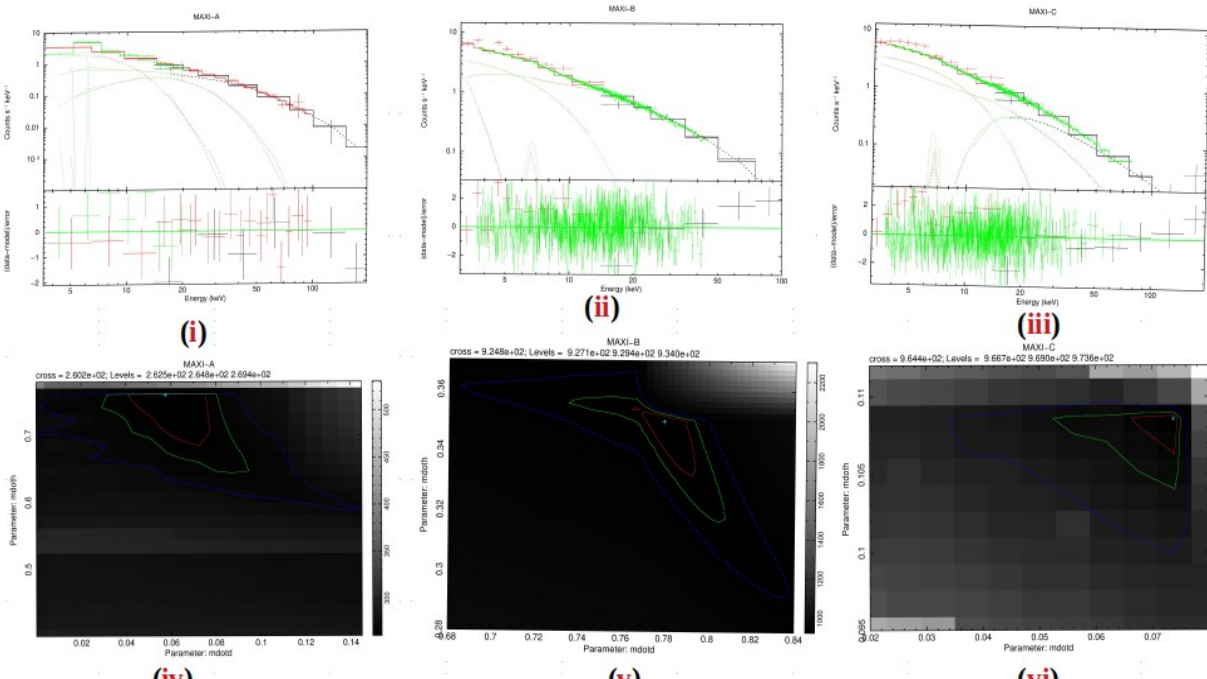


Fig. 1: Upper: X-ray spectra of MAXI J1535-571. Lower: Contour plot of $m_{dot,h}$ vs $m_{dot,d}$.

Conclusion

• The spectral results and correlation of accretion flow parameters suggests that $m_{dot,d}$ and $m_{dot,h}$ are **intrinsic properties** of the accretion flow that interact at varying distances, causing a decrease in the **ARR** as the outburst progresses. This could be responsible for the delay in **transition period** of MAXI J1535-571).

Outline;

- Introduction.
- Aim & Objectives.
- Data reduction and Analysis.
- Results/Discussion.
- Summary/Conclusion.

Aim & Specific objectives:

- Spectral analysis of MAXI J1535-571 data observed on the same and/or close-in epochs.
- Constrain physical parameters of the accretion flow, and obtain their correlations.
- Determine the variations of mass accretion rates and other accretion flow parameters and examine them.
- Determine the physical processes responsible for fluctuations and saturation effect in the accretion flow parameters, and the flickering behavior of MAXI J1535-571.
- examine the dynamic/geometry of the accretion flow, and compare the results with that of other similar sources.

R_{TCAF}	4.002 ± 0.023	$3.949^{+0.046}_{-0.046}$	3.84 ± 0.002
$norm_{TCAF}$	33.641 ± 1.045	$25.062^{+0.09}_{-0.21}$	59.012 ± 0.104
Γ_{silver}	2.13 ± 0.08	2.02 ± 0.01	2.21 ± 0.11
θ_{silver} (°)	$48.68^{+0.17}_{-0.15}$	$60.24^{+0.05}_{-0.06}$	$59.72^{+0.05}_{-0.12}$
$norm_{silver}$	7.58 ± 0.021	5.82 ± 0.124	6.214 ± 0.117
$E_{6.5,gsms}/keV$	$6.486^{+0.091}_{-0.088}$	6.500 ± 0.002	$6.521^{+0.001}_{-0.011}$
E_{silver}/keV	0.142 ± 0.015	0.102 ± 0.004	0.317 ± 0.158
$norm_{gsms}$	1.049 ± 0.001	0.540 ± 0.011	0.181 ± 0.022
χ^2	31.81	493.01	530.87

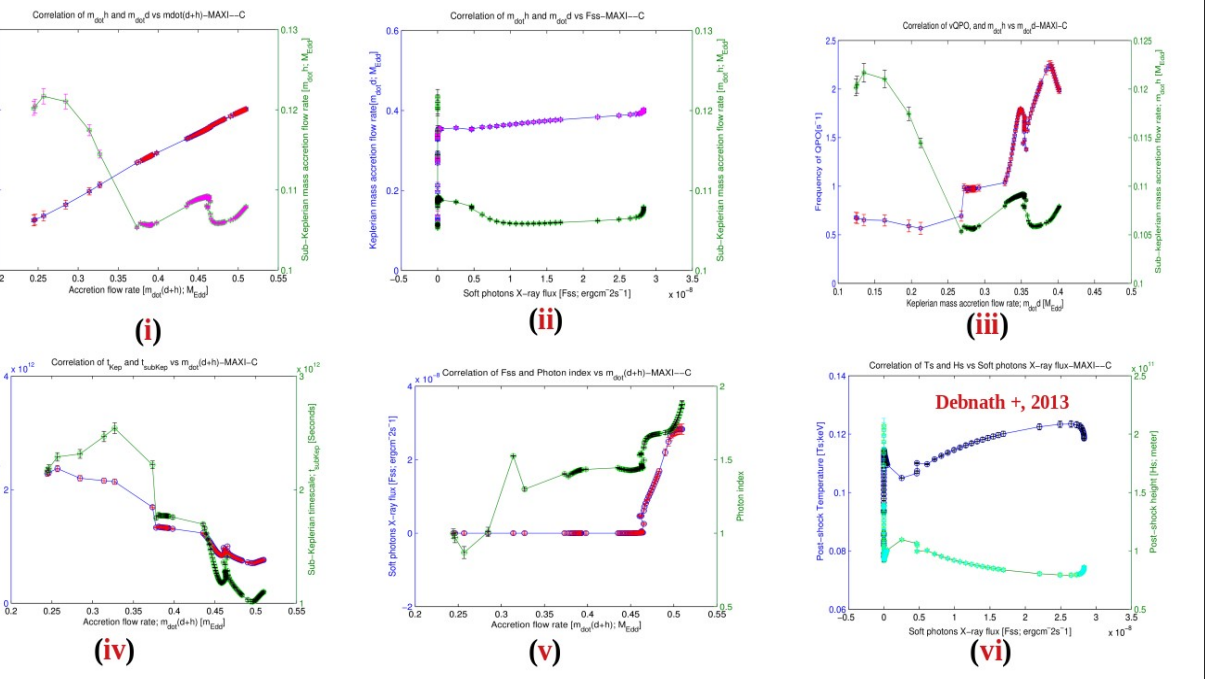
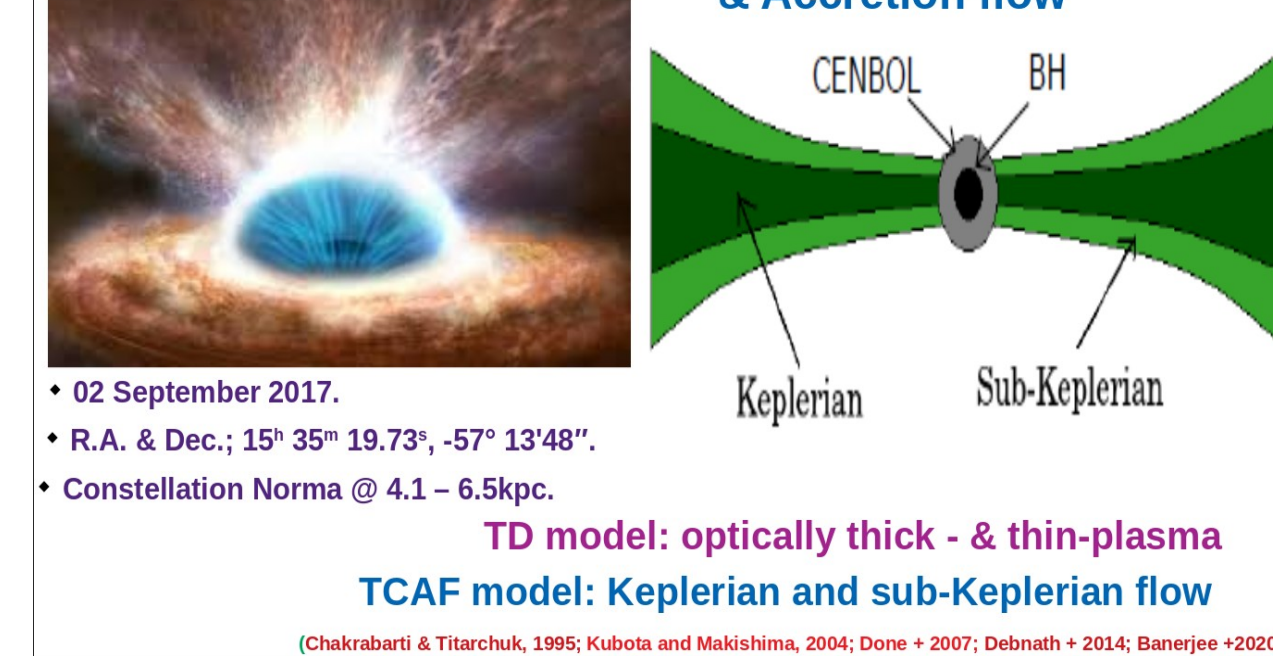


Fig. 2: Accretion flow parameters.

Introduction: MAXI J1535-571 outburst evolution & Accretion flow



Data Reduction/Analysis & Fitting/modelling

- Source of Data: MAXI/GSC, Swift/BAT, & NuSTAR; 14th Sept. 2017.
- HEASARC (https://heasarc.gsfc.nasa.gov/docs/archive.htm)
- HEASoft v6.28, mxproduct, batsurvey product, nupipeline v1.6, XSPEC v12.10.1f, etc.
- MAXI/GSC: UT 03:36:00 to 06:00:00, 17:35:59 to 19:59:59, & 04:36:00 to 21:00:00.
- Swift/BAT: 05:02:51 to 14:23:29, 05:21:58 to 14:41:58, & 05:43:54 to 20:52:58.
- NuSTAR: 05:11:09 to 13:16:09, 09:51:09 to 20:16:09, & 03:16:09 to 21:38:18
- Data reduction /Analysis
- Merge
- Spectral fitting/modelling
- $const*tbabs*(bmc*highcut+tbody+diskbb+grad+gaus)-M1$
- $const*tbabs*(nthcomp+diskbb+grad+gaus)-M2$
- $const*(PL+diskbb+grad+gaus)-M3$
- $const*tbabs*(TCAF+Xilver+gaus)-M4$
- $const*tbabs*(TCAF+nthcomp+diskbb+grad+gaus)-M5$

d.o.f	27	483	454
$rd\chi^2$	1.17	1.02	1.16
N_{hp}	2.391×10^{-01}	3.664×10^{-01}	7.311×10^{-01}

const = constant energy independent model, N_H = hydrogen absorption column density of $tbabs$ model, m_{dot,d_TCAF} = Keplerian flow mass accretion rate of TCAF model, m_{dot,h_TCAF} = sub-Keplerian flow mass accretion rate of TCAF model, m_{bb_TCAF} = mass of the black hole of TCAF model, X_S_TCAF = shock location of TCAF model, r_s = gravitational radius, R_{TCAF} = compression ratio of TCAF model, $norm_{TCAF}$ = normalization parameter of TCAF model, $E_{6.5_gsms}$ = iron emission line at 6.5 keV of $gaus$ model, E_{silver} = emission line width of $gaus$ model, $norm_{gsms}$ = normalization parameter of the $gaus$ model, Γ_{silver} = photon index of the $xilver$ model, θ_{silver} = angle of inclination of the $xilver$ model, $norm_{silver}$ = normalization parameter of $xilver$ model, χ^2 (Chi-squared) = FID/ Test statistics, d.o.f = degree of freedom, $rd\chi^2$ = reduced Chi-squared, N_{hp} = Null hypothesis probability.

Summary

- **AF: optically thin (sub-Keplerian) & optically thick (Keplerian) flow/plasma** (Chakrabarti & Titarchuk, 1995; Kubota & Makishima, 2004).
- **AF Geometry: a mix of geometrically thick and geometrically thin; dynamic** (Done + 2007; Debnath + 2015).
- **ARR ($m_{dot,h}/m_{dot,d}$) decrease from 1.4 to 0.9** → spectral evolution/transition tied to the variation of $m_{dot,d}$ and $m_{dot,h}$ (Nandi + 2012; Debnath + 2015).
- **The saturation effect occurs when the variations in $m_{dot,h}$ and $m_{dot,d}$ are not significant; an indication of converging flow observed in other galactic BHCs** (Titarchuk + 1997; Titarchuk & Seifina, 2016).

Acknowledgment

MAXI/GSC, NuSTAR, and Swift/BAT observation team for providing data and softwares, Prof. Dipak Debnath; Institute of Astronomy, Space and Earth Science, India.

Accretion Flow characteristics

- 1) Spectral properties/parameters
 - **Hard state (HS).** $1.3 \leq \Gamma \leq 1.8$ $\dot{M}_d \uparrow$, $\dot{M}_h \uparrow$ & $ARR \downarrow$
 - **Hard-intermediate state (HIMS).** $\Gamma \sim 1.8-2.3$
 - **Soft-intermediate state (SIMS).** $\Gamma = 2.3-3.0$
 - **Soft state (SS) ?**
- 2) Temporal (Timing) properties
 - **QPO A, B, & C; Indicator of changes in spectral states.**
 - **vQPOs: 1 mHz - 1 kHz**

Estimation of Accretion flow Characteristics – MATLAB

$$r_l = \left(\frac{K}{\cos \theta} \right)^{1/2} \times D_{10} \quad (1)$$

$$F_{obs} = \frac{[F_s - F_{abs}]}{2 \cos \theta} \quad (6)$$

$$F_s = 0.0165 \left[\frac{r_l \cos \theta}{D^2} \right] \left[\frac{T_s}{1 \text{ keV}} \right]^2 \times \text{photons}^{-1} \text{cm}^{-2} \quad (7)$$

$$R_l = \xi \cdot K^2 \cdot r_l \quad (2)$$

$$T = \left[\frac{3GM_{dot} M_{dot}}{8\pi\sigma r_l} \left(1 - \beta \sqrt{\frac{R_l}{r_l}} \right) \right]^{1/4} \quad (3)$$

$$F_{abs} = 2 \cos \theta \cdot r_s^2 \sigma T^4 D^2 = \frac{3GM_{dot} M_{dot} \cos \theta}{4\pi r_s D^2} (1 - \sqrt{\xi} K^2) \quad (4)$$

$$L_{abs} = 4\pi r_s^2 \sigma T^4 = \frac{3GM_{dot} M_{dot}}{2r_s} \times (1 - \sqrt{\xi} K^2) \quad (5)$$

$$L_{dot} = 2\pi D^2 \times \frac{[F_s - F_{abs}]}{\cos \theta} \quad (7)$$

$$M_{dot} = \frac{L_{dot}}{\eta c^2} = \frac{\dot{M}_{dot}}{M_{Edd}} \quad (8)$$

$$\dot{M}_E = \frac{L_E}{\eta c^2} = \frac{4\pi GM_{dot} \dot{M}_d}{\eta \sigma_T c} \quad (9)$$

T2 M5 Correlation of accretion flow characteristics

Figure	Parameter	Correlation coefficient (R)	P-value	Lower bound	Upper bound	Direction & strength of correlation
Fig.2 (i)	$m_{dot,d}$ vs $m_{dot,h}$	0.999	0.0000	0.998	1.000	Very strong positive
Fig.2 (ii)	$m_{dot,d}$ vs F_{SS_MS}	0.587	0.0000	0.435	0.707	Strong positive
Fig.2 (iii)	$m_{dot,h}$ vs F_{SS_MS}	-0.257	0.0133	-0.439	-0.055	Weak negative
Fig.2 (iv)	vQPO vs m_{dot,d_MS}	0.889	0.0000	0.836	0.925	Very strong positive
Fig.2 (v)	$m_{dot,h}$ vs m_{dot,d_MS}	-0.641	0.0000	-0.747	-0.501	Strong negative

- **Hs and Ts are anti-correlated (Fig. 2(iv))** instead decreasing with an increase in the interception of soft photons, and suppression of coronal activities (Debnath + 2013).
- This suggests flickering behavior of MAXI J1535-571 in that variations of $m_{dot,h}$ and $m_{dot,d}$ change the shape of the post-shock region periodically (Esin + 2012; Debnath + 2014).
- The variations/fluctuations of $m_{dot,d}$ and $m_{dot,h}$ created QPO (Chakrabarti & Manickam, 2000; Ingram & Done, 2011) in the accretion flow (post-shock region) when their timescales are roughly matched (Fig. iv; Molteni + 1995) as earlier noted in H 1743-322, and MAXI J1543-564 (Mondal + 2014; Chatterjee + 2016).

Recommendation

Broadband spectral analysis of the source using additional data of AsTROSAT, HXMT, and NICER alongside MAXI/GSC, NuSTAR, and Swift/BAT to elucidate this study. Also, investigation of the role of magnetic viscosity/field in driving the components of the accretion flow and transition period during the outburst evolution are paramount.

Physical Mechanisms ?

- **Hard/soft X-ray flux variability and flickering behavior.**
 - **Outburst/spectral evolution.**
 - **Oscillatory waves in the post-shock regions that produces QPO.**
 - **Fluctuation & saturation effect.**
 - **Origin of Γ -vQPO relation.**
 - **Accretion flow dynamics/geometry.**
- (Nakahira+ 2018; Tao+ 2018; Stiele & Kong, 2018; Shang+ 2019; Sreenari+ 2019; Bhargava+ 2019)

Estimation of Accretion flow Characteristics – MATLAB

$$F_{ss} = 7.6 \times 10^{26} r_s^{-3} I \left(\frac{\dot{M}_d}{M_{dot}} \right)^2 \left(\frac{\dot{M}_d}{1.4 \times 10^{17}} \right) \text{erg cm}^{-2} \text{S}^{-1} \quad (10)$$

$$T_s = \frac{m_p (R-1) c^2}{2R^2 k_B (X_s - 1)} \quad (13)$$

$$v_{app} = \frac{c}{2\pi R r_s \Gamma_s (r_s - 1)^{1/2}} = \frac{v_{so}}{2\pi R r_s \Gamma_s (r_s - 1)^{1/2}} \quad (11)$$

$$r_s = 2GM_{dot}/c^2 \quad v_{so} = c/r_s = c^2/2GM_{dot}$$

$$\tau_r = \frac{t_c}{t_i} = 3.5 \times 10^{-4} \left(\frac{1+A_r}{f_o \Gamma} \right) \left(1 - \frac{1}{R^2} \right) = 0.5 < \tau_r < 1.5 \quad (14)$$

$$H_s = \left[\frac{\gamma |R-1| X_s^2}{R^2} \right]^{1/2} \quad (12)$$

$$t_i = X_s / |V_s - R X_s| X_s^{-1/2} \quad V_s = 1/(X_s - 1)^{1/2}$$

Resonance Condition

Figure	Parameter	Correlation coefficient (R)	P-value	Lower bound	Upper bound	Direction & strength of correlation
Fig.2 (iv)	t_{app} vs $m_{dot,d}$	-0.973	0.0000	-0.982	-0.959	Very strong negative
Fig.2 (v)	t_{app} vs $m_{dot,d}$	-0.938	0.0000	-0.959	-0.908	Very strong negative
Fig.2 (vi)	F_{ss} vs $m_{dot,d}$	0.594	0.0000	0.443	0.712	Moderate positive
Fig.2 (vii)	Γ vs $m_{dot,d}$	0.847	0.0000	0.777	0.896	Very strong positive
Fig.2 (viii)	T_s vs F_{SS_MS}	0.658	0.0000	0.523	0.760	Strong positive
Fig.2 (ix)	H_s vs F_{SS_MS}	-0.536	0.0000	-0.667	-0.372	Strong negative

- **The resonance condition of $(0.62-0.79) \pm 0.04$ (Fig. 14; Chakrabarti, 2015) and best-fit photon index of 2.02-2.21 (Tao + 2018; Nakahira + 2018) affirms the presence of QPO in the accretion flow of MAXI J1535-571 during the HIMS.**
- **The value of vQPO obtained is consistent with the type-C QPO frequency; 0.1-10 Hz observed in hard states of BHCs (Motta + 2012; Mereminskiy + 2018).**
- **The variations/fluctuations of $m_{dot,d}$ and $m_{dot,h}$ in the post-shock region causes distribution of power-law energy spectral indices, and create corresponding variations/fluctuations in Γ (see Fig. 3c-e; Sunyaev & Truemper, 1979; Sunyaev & Titarchuk, 1980; Chakrabarti & Titarchuk, 1995; Yaqoob, 1997; Esin + 1998).**

Thanks for Listening